ELSEVIER

Biophysical Chemistry 98 (2002) 27–34

Biophysical Chemistry

www.elsevier.com/locate/bpc

Intramolecular electron transfer in cytochrome cd_1 nitrite reductase from *Pseudomonas stutzeri*; kinetics and thermodynamics

Ole Farver[a,*], Peter M.H. Kroneck[b], Walter G. Zumft[c], Israel Pecht[d]

[a]*Department of Analytical and Pharmaceutical Chemistry, The Royal Danish School of Pharmacy, DK-2100 Copenhagen, Denmark*

[b]*Fachbereich Biologie, Universität Konstanz, D-78457 Konstanz, Germany*

[c]*Lehrstuhl für Mikrobiologie, Universität Fridericiana, D-76128 Karlsruhe, Germany*

[d]*Department of Immunology, The Weizmann Institute of Science, 76100 Rehovot, Israel*

Received 20 September 2001; received in revised form 24 October 2001; accepted 24 October 2001

Abstract

Cytochrome cd_1 nitrite reductase from *Pseudomonas stutzeri* catalyzes the one electron reduction of nitrite to nitric oxide. It is a homodimer, each monomer containing one heme-*c* and one heme-d_1, the former being the electron uptake site while the latter is the nitrite reduction site. Hence, internal electron transfer between these sites is an inherent element in the catalytic cycle of this enzyme. We have investigated the internal electron transfer reaction employing pulse radiolytically produced *N*-methyl nicotinamide radicals as reductant which reacts solely with the heme-*c* in an essentially diffusion controlled process. Following this initial step, the reduction equivalent is equilibrating between the *c* and d_1 heme sites in a unimolecular process ($k=23\ s^{-1}$, 298 K, pH 7.0) and an equilibrium constant of 1.0. The temperature dependence of this internal electron transfer process has been determined over a 277–313 K temperature range and yielded both equilibrium standard enthalpy and entropy changes as well as activation parameters of the specific rate constants. The significance of these parameters obtained at low degree of reduction of the enzyme is discussed and compared with earlier studies on cd_1 nitrite reductases from other sources.

Keywords: Activation parameters; Conformational change; Driving force; Pathway; Pulse radiolysis; Reorganization

1. Introduction

The cd_1 nitrite reductases (EC 1.9.3.2) constitute a family of enzymes catalyzing the one-electron reduction of nitrite to nitric oxide which is an essential step in denitrification [1]. The enzyme is a homodimer of 60 kDa subunits, each containing one heme-*c* and one heme-d_1. Extensive studies have established heme-*c* as the electron entry site whereas heme-d_1 constitutes the catalytic center [2]. Three-dimensional structures of two different types of cytochromes cd_1 have so far been determined: *Paracoccus pantotrophus*, *Pp*-NiR [3], and *Pseudomonas aeruginosa*, *Pa*-NiR [4]. In both enzymes, heme-*c* is covalently linked to the N-terminal α-helical domain and heme-d_1 is bound

*Corresponding author.

E-mail address: of@dfh.dk (O. Farver).

0301-4622/02/$ - see front matter
PII: S0301-4622(02)00082-0

non-covalently to the C-terminal β-propeller domain.

Intramolecular electron transfer, ET, between *c* and d_1 hemes is an essential step in the catalytic cycle and has been studied by several groups using different methods [2,5–8]. In *Pa*-NiR the rate constants were found to be in the order of 1 s^{-1} [2,5,7]. For *Pp*-NiR intramolecular ET was found to be significantly faster with a rate constant of 1.4×10^3 s^{-1} [8]. Such a pronounced difference in rates is particularly interesting as the distances separating the two heme centers are similar (1.1 nm edge-to-edge or 2.0 nm Fe-to-Fe) in the two proteins [3,4]. Likewise, the driving forces do not reconcile such a difference in rates. Obviously, structural differences among these two cd_1-NiRs are decisive in governing the different rate constants of the intramolecular ET processes. Indeed, unexpected for such closely related enzymes, the structural details of these two proteins differ significantly: heme-*c* iron(III) in *Pp*-NiR has His/His axial ligands whereas at the heme-d_1 iron(III) the axial ligands are Tyr/His [3]. Upon reduction, the heme-*c* iron(II) ligands switch to His/Met concomitant with dissociation of the tyrosine ligand, leaving the heme-d_1 iron(II) five coordinated [9]. In contrast, heme-*c* in *Pa*-NiR is His/Met coordinated in both oxidation states while the axial heme-d_1 ligands are hydroxide and His in the oxidized state and assumed to become pentacoordinated (vacant/His, respectively), in the reduced state [10]. A remarkable feature of *Pa*-NiR enzyme is the 'arm exchange' or 'domain swapping' of the N-terminal region, which places Tyr10 of one monomer close to the heme-d_1 site of the other one. Tyr10 is hydrogen bonded by its OH group to the heme-d_1 hydroxide ligand, thereby preventing access of the substrate to the catalytic site [4]. In *Pp*-NiR, on the other hand, there is no 'domain swapping' and Tyr25 of the *c*-domain of the same monomer coordinates directly to the heme-d_1 iron [3].

Sequence comparison shows a striking difference between these two NiRs and nitrite reductase isolated from *Pseudomonas stutzeri*, *Ps*-NiR, where the N-terminal arm, including the tyrosines mentioned above, is missing [4]. The absence of this peptide stretch suggests differences in the reaction mechanism of the intramolecular ET, which we have started to pursue in the present study.

The pulse radiolysis method has proven useful for studying ET processes to/from and between active sites in multi centered redox enzymes [11]. Thus, Kobayashi et al. [8] have used pulse radiolysis in studies of cd_1-NIR from *Paracoccus pantotropha* (*Pp*-NiR). So far, no kinetic studies of intramolecular ET have been performed in *Ps*-NiR. In view of the very interesting differences in primary structure of cd_1-NIR from *Pa*, *Pp*, and *Ps* and the major differences in internal ET rates of the two former proteins, we have now investigated by the above method the ET between the *c*- and d_1-hemes in the latter protein. Here we report both kinetic and thermodynamic parameters characterizing the process in *Ps*-NiR molecules, which have been reduced by a single electron equivalent.

2. Materials and methods

Cytochrome cd_1 from *Pseudomonas stutzeri* strain ZoBell (ATCC 14405) was purified and its biochemical and spectroscopic parameters were characterized as described in Cheesman et al. [12].

Pulse radiolysis experiments were carried out using the Varian V-7715 linear accelerator of the Hebrew University in Jerusalem. Electrons accelerated to 5 MeV were employed using pulse lengths in the range from 0.1 to 1.5 μs in argon saturated solutions containing 5 mM *N*-methyl nicotinamide (NMNA), 5 mM phosphate, 0.1 M *tert*-butanol, pH 7.0. All optical measurements were carried out anaerobically, under purified argon at a pressure slightly in excess of 1 atm in a 1 cm Spectrosil cuvette. A 150-W xenon lamp produced the analysing light beam, and appropriate optical filters with cut-off at 385 nm were used to avoid photochemistry and light scattering. The data acquisition system consisted of a Tektronix 390 A/D transient recorder and a PC. In each experiment 2000 data points were collected, divided equally between two different time scales. Usually the processes were followed over at least three half-lives. Each kinetic run was repeated at least four times. The data were fitted to a sum of exponentials using a nonlinear least squares pro-

gramme written in MATLAB®. The temperature of the reaction solutions was controlled by a thermostating system, and continuously monitored by a thermocouple attached to the cuvette. All reactions were performed under pseudo-first order conditions, with typically a tenfold excess of oxidized protein over reductant. Several pulses were applied to each protein solution, but the number of reducing equivalents introduced during the experiments never exceeded one pr. molecule All chemicals were of analytical grade and used without further purification. Milli-Q water was used throughout the studies.

3. Results

When argon saturated aqueous solutions of NMNA and *tert*-butanol are subjected to microsecond pulses of 5 MeV accelerated electrons, a series of chemical reactions is induced leading to the production of the uncharged NMNA* radicals within microseconds. The transient formation and decay of the NMNA* radicals could be followed at 420 nm where they exhibit sufficiently strong absorbance ($e_{420} = 3200\ M^{-1}\ cm^{-1}$) [8]. When *Ps*-NiR is added to the above solutions, an enhanced decay of NMNA* is observed concomitantly with the appearance of an absorption increase at ~554 nm, a characteristic wavelength for heme-*c* reduction (Fig. 1a, left panel). The small *decrease* in absorbance at 460 nm (Fig. 1b, left panel) which occurs on the same time scale as the above increase at 554 nm is due to the absorption tail of the transient NMNR* decay. A parallel bimolecular reduction of the heme-d_1 center by $NMNA^*$ would have given rise to an absorption *increase* at 460 nm, but no such process was observed (Fig. 1b). Similarly, at 670 nm where heme-d_1 reduction can also be monitored, hardly any absorption changes were observed in this faster time domain (Fig. 1d, left panel). We therefore conclude that only heme-*c* is reduced directly by $NMNA^*$ in an essentially diffusion controlled process, with a second order rate constant of $1\times10^9\ M^{-1}\,s^{-1}$ at pH 7.0 and 298 K, while no direct reduction of heme-d_1 by the radicals is taking place. It should be noted that in the present study the number of pulses introduced into the protein solution was limited so that

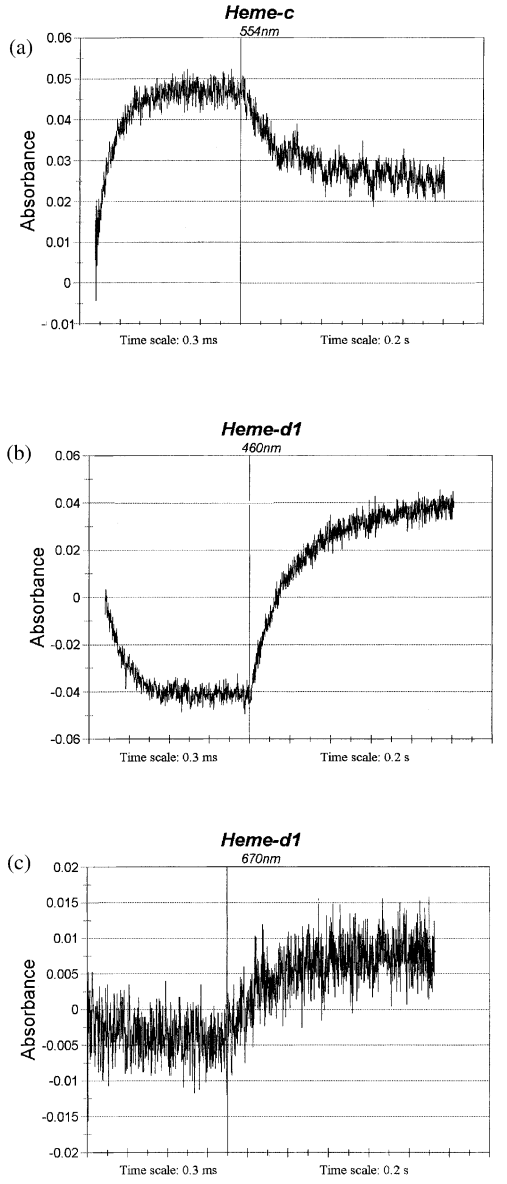

Fig. 1. Time resolved absorption changes. Concentration of *Ps*-NiR was 24 μM; 5 mM NMNA; 5 mM phosphate; 0.1 M *tert*-BuOH; Argon saturated. pH was 7.0 and the temperature was 298 K. Optical path length 1.0 cm; Pulse width 1.0 μs. (a) Measurements at 554 nm, monitoring heme-*c* reduction (left panel:fast time scale) and heme-*c* reoxidation (right panel: slow time scale). (b) Measurements at 460 nm, monitoring tail of NMNA* decay (left panel: fast time scale) and heme-d_1 reduction (right panel: slow time scale). (c) Measurements at 670 nm, monitoring heme-d_1 reduction (right panel: slow time scale).

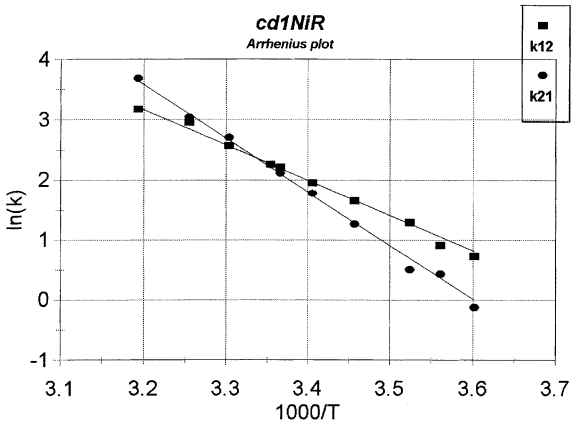

Fig. 2. Temperature dependence of the individual rate constants for intramolecular ET in *Ps*-NiR. The rate constants, k_{12} and k_{21}, are defined in Eq. (1).

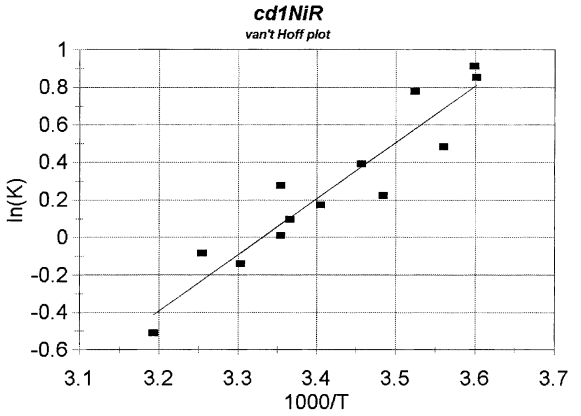

Fig. 3. Temperature dependence of the intramolecular ET equilibration. The equilibrium reaction is defined in Eq. (1).

the enzyme molecules did not take up more that one electron equivalent.

Following the above direct heme-*c* reduction, a decrease in the 554 nm absorption was observed on a slower time scale (Fig. 1a; right panel) indicating *reoxidation* of the heme-*c* Fe(II) center. Concomitantly, absorption increases were monitored at both 460 nm (Fig. 1b; right panel) and 640 nm (Fig. 1c; right panel) where, as stated above, reduced heme-d_1 has strong absorption bands. The rate constant for this process was determined to be $k_{ET}=23\ s^{-1}$ at 298 K and pH 7.0, independent of NMNA* and initial protein concentration, implying that a unimolecular reaction takes place, namely intramolecular ET between heme-*c* and heme-d_1. Analysis of the reaction amplitudes, however, made it clear that the internal electron transfer processes do not proceed to completion: at 298 K, only 50% of the electrons initially taken up by oxidized heme-*c* were transferred to heme-d_1 Fe(III), consistent with an equilibrium constant for Eq. (1) of 1.0.

$$\text{heme-}c\ \text{Fe(II)}\ \text{heme-}d_1\ \text{Fe(III)} \underset{k_{21}}{\overset{k_{12}}{\rightleftarrows}} \text{heme-}c\ \text{Fe(III)}\ \text{heme-}d_1\ \text{Fe(II)} \quad (1)$$

The observed rate constant, k_{ET}, is the sum of rate constants for the forward and back ET reactions: $k_{ET}=k_{12}+k_{21}$. Combining the observed rate and equilibrium constants it is now possible to extract rate constants for the individual processes.

We have investigated the intramolecular ET reaction over a relatively broad temperature range (4–40 °C) and have determined both activation and thermodynamic parameters of the reactions (Figs. 2 and 3). Table 1 summarizes all observed rate and equilibrium data.

Table 1
Kinetics and thermodynamics of heme-*c* heme-d_1 intramolecular ET process in *Ps*-NiR

Kinetic parameters	k/s^{-1} (298 K)	$\Delta H^{\neq}$/kJ mol^{-1}	$\Delta S^{\neq}$/J K^{-1} mol^{-1}
Forward, k_{12}	11.7±1	46.2±4.8	−71.0±1.5
Back, k_{21}	11.3±1	71.6±4.8	+13.6±1.5
Equilibrium data	K	ΔH^0/kJ mol^{-1}	ΔS^0/J K^{-1} mol^{-1}
	1.0±0.1	−24.9±2.5	−83±8.4

Table 2
Rate constants for inramolecular ET in nitrite reductases from different sources

Source	k_{ET}/s^{-1}	Conditions	Reference
Paracoccus pantotrophus	1400	pH 7.0	[8]
Pseudomonas aeruginosa	0.3	pH 7.0; 298 K	[7]
Pseudomonas aeruginosa	0.25	pH 7.0; 298 K	[5]
Pseudomonas stutzeri	23	pH 7.0; 298 K	This work

4. Discussion

A key challenge in studies of biological redox processes is trying to define and understand the parameters which control the rates of ET. These parameters include, (i) driving force, i.e. change in free energy of the reaction; (ii) the reorganization energy, i.e. the energy of the reactants at the equilibrium nuclear configuration of the products; (iii) the distance separating electron donor and acceptor; and finally (iv) the nature of the medium separating the two redox centers.

It is of interest to compare the rate constants determined here for the intramolecular ET in *Ps*-NiR, 23 s^{-1} at 298 K, pH 7.0, with the corresponding rate constants reported for *Pa* and *Pp*-NiR's (cf. Table 2). An early stopped-flow study of the reduction kinetics of *Pa*-NiR by an excess of reduced azurin yielded a rate constant of 0.25 s^{-1} at pH 7.0 and 298 K [5]. In another stopped-flow study on *Pa*-NiR, Silvestrini et al. [2] determined a rate constant of 1 s^{-1} at 293 K and pH 8 for the reduction. Schichman and Gray [7] have performed stopped-flow measurements on *Pa*-NiR using $Fe(EDTA)^{2-}$ as reductant and obtained a rate constant of 0.3 s^{-1} at pH 7.0 and 298 K. Kobayashi et al. [8], employing pulse radiolysis to study the intramolecular heme-*c* to heme-d_1 ET in *Pp*-NiR reported a considerably larger rate constant, 1.4×10^3 s^{-1} at pH 7.0. Furthermore, they observed an essentially quantitative transfer of electrons from the reduced heme-*c* to oxidized heme-d_1 implying an equilibrium constant, which is far from unity. Thus, the rates determined in the present study for *Ps*-NiR lie in between those observed for the two other nitrite reductases. This raises the question of what is the cause(s) for such a pronounced difference in reactivity among enzymes closely related in structure and performing an identical catalytic process.

Driving force is one parameter determining rates of ET. In the absence of external ligands, the reduction potentials of heme-*c* and heme-d_1 in *Pa*-NiR are similar, $\sim$280 mV [7]. In contrast, the observed irreversibility of the intramolecular $c \rightarrow d_1$ ET in *Pp*-NiR indicates that the difference in reduction potentials between these sites must be larger than 100 mV [8]. Results of our study of this equilibrium in *Ps*-NiR are in line with those of *Pa*-NiR, as we find the equilibrium constant to be 1.0 at 298 K and pH 7.0, an observation excluding differences in driving force as being responsible for the observed hundred fold faster rate in the intramolecular ET in *Ps*- compared with *Pa*-NiR. Rather, the causes for the distinct rates could be subtle differences in the nature of the separating media (i.e. the ET pathway) and/or different reorganization energies. Still, the higher driving force in *Pp*-NiR would contribute to a faster rate of intramolecular ET in this enzyme compared with that in the *Ps*-NiR.

We will therefore focus on the structural aspects. As already mentioned above it is noteworthy that the distances separating the *c* and d_1 heme centers are similar (1.1 nm edge-to-edge or 2.0 nm Fe-to-Fe) in the two proteins [3,4] The heme-d_1 binding domains are quite similar in the three-dimensional structures of oxidized *Pa*- and *Pp*-NiR with one interesting exception: the sixth ligand in *Pa*-NiR is a hydroxide ion which is hydrogen bonded to a tyrosine, Tyr10, belonging to the N-terminal stretch of the second monomer [4]. In *Pp*-NiR a tyrosine, Tyr25, of the same monomer is coordinated directly to Fe(III) [3]. No homologous tyrosines are present in the *Ps*-NiR sequence [13]. The oxidized heme-*c* domains of *Pa*- and *Pp*-NiR also differ in

their axial ligands: *Pa*-NiR exhibits the classical coordination by His and Met [4], while the latter ligand is replaced by a His in the *Pp* enzyme [3]. It has been shown by MCD and EPR spectroscopy that in the oxidized state, heme-*c* of *Ps*-NiR has His/Met axial ligation as in *Pa*-NiR while studies of the heme-d_1 suggest that the axial ligands are His/Tyr or possibly His-hydroxide [12].

Following reduction, major conformational changes are observed in *Pp*-NiR where one His ligand of heme-*c* is replaced by a Met and the Tyr ligand dissociates from the heme-d_1 iron coordination sphere [9]. In *Pa*-NiR, much smaller conformational alterations take place [10]: reduction of the *c*-heme is not accompanied by axial His/Met ligands change, and at the heme-d_1, reduction and hydroxide ion dissociation are closely linked, thereby providing access to external ligands like oxidizing substrates. Thus, the much higher rate of intramolecular ET in *Pp*-Nir compared with *Pa*-NiR could be due to the inability of heme-d_1 in the latter enzyme to accept an electron while the hydroxide is still coordinated to the iron(III) center. This makes the dissociation of the OH^- ligand rate limiting for the ET. Indeed, this notion is supported by X-ray structural work on *Pa*-NiR with a reduced heme-*c* and an oxidized heme-d_1 where the latter still binds the hydroxo ligand [14].

The three-dimensional structure of *Ps*-NiR has not yet been determined, but sequence comparison demonstrates a high degree of homology with the two other cd_1 nitrite reductases [4]. Still, one major difference between *Pa*- and *Ps*-NiR sequences should be stressed, since it probably bears significant consequences for the reactivity of the proteins: the N-terminal arm of *Pa*-NiR is wrapped around the d_1-domain of the second monomer, and Tyr10 of this segment is hydrogen bonded to the hydroxide ligand of heme-d_1 [4]. Obviously, without this N-terminal extension in *Ps*-NiR, ET pathways must be significantly different in the two proteins.

In studies of the photodissociation of CO from fully reduced *Pa*- and *Ps*-NiR, evidence for fast global structural changes has been obtained [15], probably excluding a major role for the extended N-terminal peptide in this process. On a much slower time scale, a second transient decay has been observed in *Ps*-NiR, with a rate constant of 8 s^{-1}. It is not clear whether this rate is independent of CO concentration, but it is noteworthy that the rate of this conformational change is quite similar to that of the ET observed here for *Ps*-NiR. The challenge now is to try and identify the nature of this process. A better understanding will obviously depend on acquiring the three-dimensional structure of this protein.

It is interesting to compare rate constants and activation parameters of the intramolecular ET in *Ps*-NiR with those determined for analogous intramolecular ET processes in other multicenter redox enzymes. We have previously studied the reversible intramolecular ET between type 1 and type 2 sites in a copper-containing nitrite reductase from *Alcaligenes xylosoxidans* (CuNiR) [16]. The rate constant for type 1 Cu(I) to type 2 Cu(II) ET was found to be 185 s^{-1}, i.e. ten fold faster than in *Ps*-NiR. When we compare the activation parameters of the two processes, the cause for this difference becomes obvious: the activation enthalpy for the CuNiR process is much smaller (22.7 kJ mol^{-1}) suggesting that structural reorganization apparently plays a much smaller role, as it is limited by the rigid β-sheet structured copper enzyme. The equilibrium constant of internal ET in the latter protein is 0.7 at 298 K indicating a slight 'uphill' reaction with type 2 Cu(II)/(I) having the higher reduction potential [16].

We have also studied the intramolecular electron transfer in bovine cytochrome *c* oxidase (COX) by the pulse radiolysis method where the rate constant of ET from reduced Cu_A (I) to oxidized Fe(III) heme-*a* is significantly faster, in spite of a considerably larger distance separating the donor and acceptor (2.5 nm): $k = 1.3 \times 10^4$ s^{-1} for the forward reaction at 298 K and pH 7.0. As with CuNiR this faster rate is due to an even more favorable activation enthalpy term (11.4 kJ mol^{-1}) [17].

It seems plausible that the much slower intramolecular ET rate constants in *Ps*-NiR compared with COX are due to a reorganization step involving considerable structural changes such as those leading to ligand substitution in the coordination spheres of the hemes. In *Pa*-NiR, reduction of heme-d_1 requires dissociation of the hydroxide ion ligand as suggested above. ET from heme-*c* to

heme-d_1 is possibly governed by dissociation of this OH^- ligand, which could indeed be the built-in mechanism for control of ET rates. A similar gating mechanism could apply to *Ps*-NiR. The activation parameters determined for the intramolecular ET processes demonstrate some noteworthy features. Particularly the difference between activation entropies for heme-d_1 reduction [Scheme 1, see Eq. (1), process 12] and reoxidation (Scheme 1, process 21) deserves attention: examining the d_1-heme pocket in *Pa*-NiR, a channel could be identified composed of polar side chains and main chain atoms [4]. It has been shown that the Tyr10 side chain in *Pa*-NiR rotates upon heme-d_1 reduction, leaving the catalytic site open for ligand binding [10], either substrates or solvent molecules. This would lead to an expected decrease in activation entropy as indeed observed here for *Ps*-NiR. Upon reoxidation and release of exogenous ligands like reaction products or water molecules this site closes again thus causing an increase in activation entropy. This is again in accordance with our observations (Table 1).

The above results provide initial insights into the intricate control which may be extended to internal ET processes in enzymes catalyzing multistep processes. Further detailed analysis of the control of the ET during complete reductive titrations of *Ps*-NiR are currently in progress.

Acknowledgments

This paper is dedicated to Professor Maurizio Brunori on the occasion of his 65th birthday. IP and PK wish to thank the Volkswagen Stiftung and the German Israeli Foundation for ongoing support. WZ thanks the Deutsche Forschungsgemeinschaft and Fonds der Chemischen Industrie for financial support. OF acknowledges financial support from the Danish Natural Science Research Council.

References

[1] W.G. Zumft, Cell biology and molecular basis of denitrification, Microbiol. Mol. Biol. Rev. 61 (1997) 533–616.

[2] M.C. Silvestrini, M.G. Tordi, G. Musci, M. Brunori, The reaction of *Pseudomonas* nitrite reductase and nitrite, J. Biol. Chem. 265 (1990) 11783–11787.

[3] V. Fülöp, J.W.B. Moir, S.J. Ferguson, J. Hajdu, The anatomy of a bifunctional enzyme: structural basis for reduction of oxygen to water and synthesis of nitric oxide by cytochrome cd_1, Cell 81 (1995) 369–377.

[4] D. Nurizzo, M.-C. Silvestrini, M. Mathieu, F. Cutruzzola, D. Bourgeois, V. Fülöp, J. Hajdu, M. Brunori, M. Tegoni, C. Cambillau, Structure 5 (1997) 1157–1171.

[5] S.R. Parr, D. Barber, C. Greenwood, The electron-transfer reaction between azurin and the cytochrome *c* oxidase from *Pseudomonas aeruginosa*, Biochem. J. 167 (1977) 447–455.

[6] Y. Blatt, I. Pecht, Allosteric cooperative interactions among redox sites of *Pseudomonas* cytochrome oxidase, Biochemistry 18 (1979) 2917–2922.

[7] S.A. Schichman, H.B. Gray, Kinetics of the anaerobic reduction of ferricytochrome cd_1 by $Fe(EDTA)^{2-}$. Evidence for bimolecular and intramolecular electron transfer to the d_1 hemes, J. Am. Chem. Soc. 103 (1981) 7794–7795.

[8] K. Kobayashi, A. Koppenhöfer, S.J. Ferguson, S. Tagawa, Pulse radiolysis studies on cytochrome cd_1 nitrite reductase from *Thiosphaera pantotropha*: evidence for a fast intramolecular electron transfer from *c*-heme to d_1-heme, Biochemistry 36 (1997) 13611–13616.

[9] P.A. Williams, V. Fülöp, E.F. Garman, N.F.W. Saunders, S.J. Ferguson, J. Hajdu, Haem-ligand switching during catalysis in crystals of a nitrogen-cycle enzyme, Nature 389 (1997) 406–411.

[10] D. Nurizzo, F. Cutruzzola, M. Arese, D. Bourgeois, M. Brunori, C. Cambillau, M. Tegoni, Conformational changes occurring upon reduction and NO binding in nitrite reductase from *Pseudomonas aeruginosa*, Biochemistry 37 (1998) 13987–13996.

[11] I. Pecht, O. Farver, Pulse radiolysis: a tool for investigating long-range electron transfer in proteins, in: J.F. Wishart, D.G. Nocera (Eds.), Photochemistry and Radiation Chemistry, Advances in Chemical Series 254 (1998) 65–80.

[12] M.R. Cheesman, S.J. Ferguson, J.W.B. Moir, D.R. Richardson, W.G. Zumft, A.J. Thomson, Two enzymes with a common function but different heme ligands in the forms as isolated. Optical and magnetic properties of the heme groups in the oxidized forms of nitrite reductase, cytochrome cd_1, from *Pseudomonas stutzeri* and *Thiosphaera pantotropha*, Biochemistry 36 (1997) 16267–16276.

[13] A. Jüngst, S. Wakabayashi, H. Matsubara, W.G. Zumft, The nirSTBM region coding for cytochrome cd_1-dependent nitrite respiration of *Pseudomonas stutzeri* consists of a cluster of mono-, di-, and tetraheme proteins, FEBS Lett. 279 (1991) 205–209.

[14] D. Nurizzo, F. Cutruzzola, M. Arese, D. Bourgeois, M. Brunori, C. Cambillau, M. Tegoni, Does the reduction of *c* heme trigger the conformational change of crystalline nitrite reductase?, J. Biol. Chem. 274 (1999) 14997–15004.

[15] E.K. Wilson, A. Bellelli, F. Cutruzzola, W.G. Zumft, A. Gautierrez, N.S. Scrutton, Kinetics of CO binding and CO photodissociatrion in *Pseudomonas stutzeri* cd_1 nitrite reductase: probing the role of extended N-termini in fast structural relaxation upon CO photo dissociation, Biochem. J. 355 (2001) 39–43.

[16] O. Farver, R.R. Eady, Z.H.L. Abraham, I. Pecht, The intramolecular electron transfer between copper sites of nitrite reductase: a comparison with ascorbate oxidase, FEBS Lett. 436 (1998) 239–242.

[17] O. Farver, Ö. Einarsdóttir, I. Pecht, Electron transfer rates and equilibrium within cytochrome *c* oxidase, Eur. J. Biochem. 267 (2000) 950–954.